Korean Journal of Remote Sensing, Vol.18, No.5, 2002, pp.255~261

Estimation of Instantaneous Sea Level Using SAR Interferometry

Sang-Wan Kim and Joong-Sun Won

Department of Earth System Sciences, Yonsei University

Abstract : Strong and coherent radar backscattering signals are observed over oyster sea farms that consist of artificial structures installed on the bottom. We successfully obtained 21 coherent interferograms from 11 JERS-1 SAR data sets even though orbital baselines (up to 2 km) or temporal baselines (up to 1 year) were relatively large. The coherent phases preserved in the sea farms are probably formed by double bouncing from sea surface and the sea farming structures, and consequently they are correlated with tide height (or instantaneous sea level). Phase unwrapping is required to restore the absolute sea level. We show that radar backscattering intensity is roughly correlated with the sea surface height, and utilize the fact to determine the wrapping counts. While the SAR image intensity gives a rough range of absolute sea level, the interferometric phases provide the detailed relative height variations within a limit of 2π (or 15.3 cm) with respect to the sea level at the moment of the master data acquisition. A combined estimation results in an instantaneous sea level. The radar measurements were verified using tide gauge records, and the results yielded a correlation coefficient of 0.96 with an r.m.s. error of 6.0 cm. The results demonstrate that radar interferometry is a promising approach to sea level measurement in the near coastal regions.

Key Words : Interferometry, Instantaneous sea level, Sea farm, SAR.

1. Introduction

SAR interferometry (InSAR) has been applied successfully to the observation of subtle crustal deformation induced by earthquakes, volcanic activity, aquifer systems, and etc. (Massonnet *et al.*, 1993; Amelung *et al.*, 1999; Sandwell *et al.*, 2000). SAR imagery has also provided many valuable oceanographic features such as internal waves, eddies and currents, surface wind stress, and oil slicks. However, the radar interferometry has not be considered applicable to the sea surface, while satellite radar altimetry such as TOPEX-POSEIDON has been used to measure sea surface height (Robinson, 1995; Schmullius and Evans, 1997). The satellite altimetry is, however, not reliable in the near coast. Recently, Alsdorf *et al.* (2000, 2001a, 2001b) studied the Amazon flood plain using L-band HH-polarization SAR systems and succeeded in demonstrating that interferometric phases were correlated with changes in the river. The water surface in the flood plain studied by Alsdorf is characterized by smooth surface and very slow varying water level. In

Received 20 August 2002; Accepted 25 September 2002.

our previous work (Kim *et al.*, 2002b), we showed for the first time that interferometric pairs can be obtained even over the rough sea surface around oyster sea farms. The sea surface is very rough and the change in water level is faster and larger than the water in flood plain. Consequently, the radar interferometry over the sea surface is by far more difficult. Although we succeeded in the generating interferograms, the accuracy of the estimated sea level in our previous work was not practically acceptable.

Along the south coast of the Korean Peninsula, a large number of sea farms are being operated. The structure of our interest is an oyster sea farm. The individual structure unit consists of a horizontal and two vertical wood bars attached on the bottom and staying about 1 ~2 m above seawater. The diameter of the bar is about 10 cm. Each oyster farm site is normally composed of fifty to one hundred units in array. These structures are undetectable by satellite optical remote sensing systems except extremely high resolution system such as IKONOS. On the contrary, SAR well images the artificial structures under favorable conditions (Fig. 1). Especially L-band HH-polarization SAR system is most effective and reliable to produce radar interferometric pairs. The returned radar signal from the oyster farming structure is as coherent as that from land. In this paper, we present the results of JERS-1 SAR interferometric application to the estimation of instantaneous sea level in the bay of Kaduckdo, Korea. Instead of open sea, we applied InSAR to the seawater in a bay in which water surface is smooth. We will show a possible InSAR technique for measuring instantaneous sea level. The radar measurements is to be verified by in-situ data recorded by a tide gauge (model: OTT-R20) installed near the study area (Fig. 1).

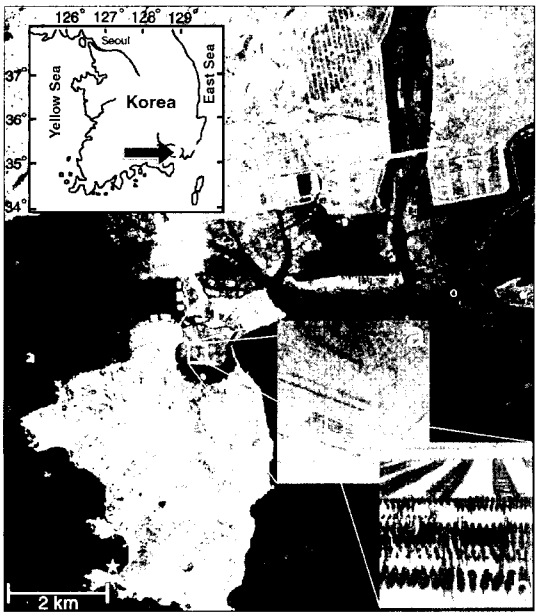

Fig. 1. Location map and the JERS-1 SAR image in radar coordinates. The sea farms and sandbars are marked by red and green dots, respectively. The blue star denotes the tide gauge station. (a) The IKONOS image is overlaid to show the structures by courtesy of e-HD.com. (b) Photograph shows the oyster farming structures.

2. Processing

As shown in Fig. 1, the oyster farms are imaged as bright scatterers by JERS-1 L-band SAR. The target structures are the oyster farms inside the bay. The interferometric phase is coherent as seen in the averaged coherence map (Fig. 2b). One can see the phase difference between land mass and water surface in Fig. 2c. The pattern of interferometric phase inside the bay is smooth and slow varying. The coherent phases are probably induced by double bounced backscattering after being reflected on the water surface first. It is similar to the inundated vegetation introduced by Alsdorf *et al.* (2000) except horizontal bars of the structure. For the study, we obtained 11 JERS-1 SAR data sets between May 2 1996 and July 3 1998, and 21 interferometric pairs were successfully generated from them. Table 1 illustrates the time intervals of the

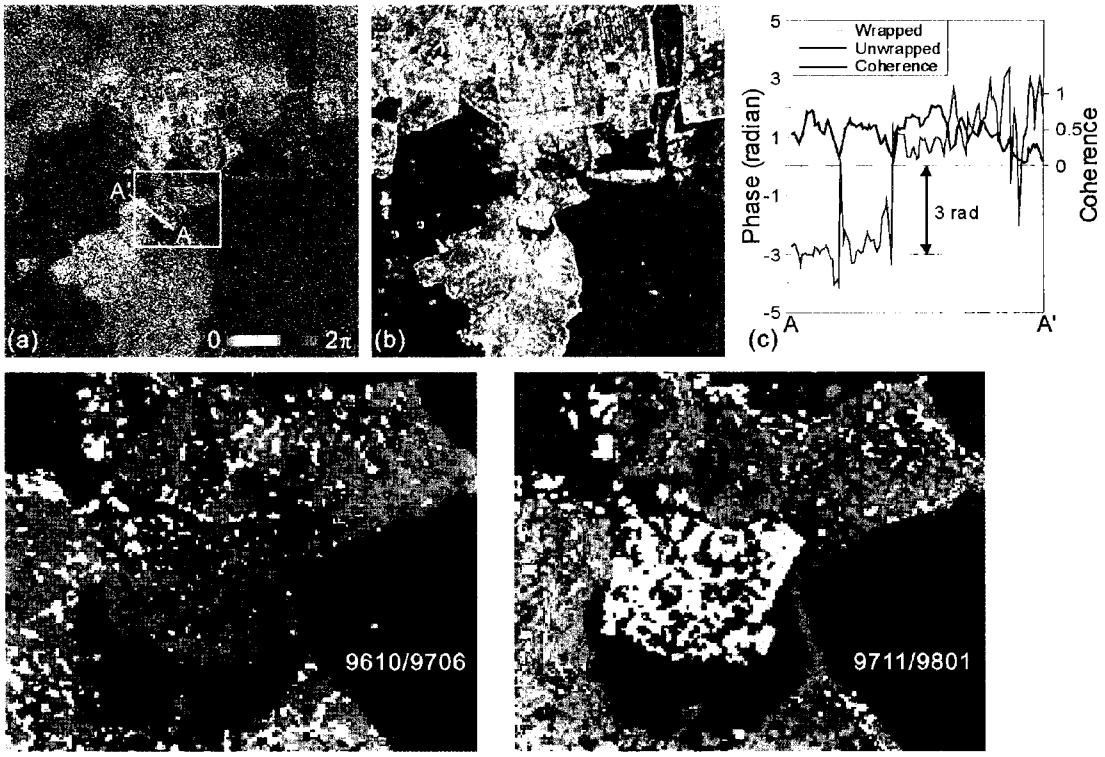

Fig. 2. (a) Differential interferogram of 9605/9606 pair. (b) Averaged coherence of 21 interferometric pairs. (c) Profile of phase and coherence along the line A-A'.

interferometric pairs, the altitude of ambiguity (h_a defined by Massonnet *et al.* (1998)), and the difference of tide height recorded by a tide gauge.

1) Differential Interferograms

Because the sea level change is regional and the surface is relatively flat, the topographic phase removal in the two-pass or three-pass DInSAR processing is not so critical as for land mass. Provided a reference phase (θ_{ref}) and height (H_{ref}) on a selected ground point and a reference sea level (H_{water}) of the master scene are known, the relative sea level change (Δz) can be formulated as the following equations:

$$e^{i\theta_d} = e^{i\theta_{ref}} \cdot e^{i\frac{H_{water}-H_{ref}}{h_a}2\pi} \cdot e^{-i\theta_{water}}, \quad (1)$$

$$\Delta z = \frac{\lambda\theta_d}{4\pi\cos(\theta_{inc})}, \quad (2)$$

where λ is the wavelength of SAR signal, and θ_{inc} is an incidence angle. Therefore, a DEM may not be necessary for the processing.

The phase due to the curvature of the earth have to be removed using orbital information. Therefore an accurate baseline is required but the accuracy of the JERS-1 orbit data are too poor to be used directly. The orbits could be further finely tuned by applying a two-pass differential processing to the neighboring land surface so that a flat earth phases and topographic phases be removed. The idea of the processing is to minimize residual phases over land mass. National digital maps of 1:25,000 scale were used for the two-pass DInSAR. To improve the baseline accuracy, we adopted the method described by Kim *et al.* (2002a). For the H_{water} value of Eq. (1), we used the tide gauge data recorded in the Kadukdo. The tide gauge data is,

Table 1. Summary of JERS-1 Interferometric Pairs.

No.	SAR image		Ambiguity	Time interval	Tide Height
	Master	Slave	Height(ha)	(days)	Difference(cm)
1	96/05/02	96/06/15	4101.3	44	11
2	96/05/02	97/01/21	151.0	264	11
3	96/05/02	97/06/02	174.9	396	-20
4	96/06/15	96/10/25	258.6	132	-12
5	96/06/15	97/01/21	-148.3	220	0
6	96/06/15	97/06/02	180.6	352	-31
7	96/10/25	97/01/21	-97.6	88	12
8	96/10/25	97/06/02	-215.0	220	-19
9	97/01/21	97/06/02	108.9	132	-31
10	97/06/02	98/05/20	-67.3	352	14
11	97/10/12	97/11/25	-34.8	44	26
12	97/11/25	98/01/08	-79.8	44	-11
13	97/11/25	98/02/21	-264.2	88	16
14	97/11/25	98/07/03	283.4	220	14
15	98/01/08	98/02/21	107.9	44	27
16	98/01/08	98/05/20	-33.8	132	-1
17	98/01/08	98/07/03	72.7	176	25
18	98/02/21	98/05/20	-26.3	88	-28
19	98/02/21	98/07/03	184.5	132	-2
20	98/05/20	98/07/03	21.7	44	26
21	96/05/02	96/10/25	262.1	176	-1

however, only an approximation to the true H_{water} because it is located about 5 km away from the test bay and SAR observation is an instantaneous sea level rather than averaged sea level recorded by the tide gauge. The small altitude ambiguity is preferred to reduce the error caused by an inaccurate H_{water}.

Resulting interferometric phase of seawater reveals nearly flat fringe pattern and is different from that of land mass. For example, Fig. 2a is a differential interferogram of the 9506/9606 pair. Even though topographic phase was eliminated, residual phases on the reclaimed ground caused by subsidence of reclaimed costal land (Kim *et al.*, 2002b) and atmospheric artifact were observed. The phase profile of Fig. 2c shows phase difference of 3 radians from land mass, which clearly indicates the change in relative sea level. However, the interferometrically measured instantaneous sea level has a sign ambiguity and an unwrapping problem. For an instance, Fig. 2c can be interpreted as 7.3 cm up welling or 8.0 cm down welling. Additional integer multiples of ± 15.3 cm are also possible, and the number of wrapping cannot be estimated from the interferogram because the phase in water surface is isolated. Therefore, the number of wrapping (or phase unwrapping) is needed to be determined by other methods.

2) Backscattering Intensity

The absolute sea level cannot properly be restored by interferometric phases alone because of the discontinuity of phase and the large sea level changes (more than about 15.3 cm in height or 2π in phase) in the area of interest. The wrapped differential phases are limited to an estimation of -7.6~7.6 cm changes due to uncertainty of sign (up or down). If the sea level change exceeds 15.3 cm, it is necessary to do phase unwrapping in order to resolve the inherent 2π ambiguity. TOPEX-POSEIDON altimetry or consecutive phase within a transition zone can be used for phase unwrapping (Alsdorf *et al.*, 2001a, 2001b). In our case, the sea level change was caused by tide that is a time harmonic function of spatially different values, thus altimetry data cannot be used to resolve the ambiguity. In addition, satellite altimetry is usually not very accurate at near coast.

The wrapped phase in land can be unwrapped since the differential phase is continuous to the displacement free area. On the contrary, the differential phase on the sea farms is isolated and disconnected from phase of surrounding sea. Consequently, we cannot determine the wrapping counts from differential interferogram. We have overcome the ambiguity problem to some extent by exploiting radar backscattering intensity (that is proportional to the image brightness). Compared to interferometry, the advantage of the approach is its ability to directly determine the surface height change if the backscattering intensity is proportional to the sea level. The intensity of radar backscattering is usually not

a function of single parameter or the length of the exposed bar, because of Bragg scattering in seawater surface. Therefore, the backscattering intensity does not provide an accurate value of absolute sea level. However, it is still useful to determine the range of wrapping counts. If corner reflection at vertical bars contributes significantly to the backscattered signals, the intensity will reflect the absolute sea level. Since an accurate sigma naught could not be estimated from JERS-1 SAR (Shimada, 1998), a normalized image intensity R can be defined by

$$R = (I_{farm} - I_{seawater}) / (I_{urban} - I_{seawater}). \quad (3)$$

where I is the peak value of fitted Rayleigh distribution, and their coefficient of determination (Ross, 1987) are all over 0.95. Backscattering intensity does not have a perfect linear relationship with sea level because it is governed by sea surface conditions, oysters growing, and etc. as well as sea level. The normalized intensity, R, was inversely proportional to the tide gauge data with a correlation coefficient of -0.83 and an r.m.s. error of 7.85 cm (Fig. 3). The results are not accurate enough to determine instantaneous sea level straightforwardly. However, the r.m.s. error must be good enough to determine the range of wrapped phase. Differential phase of the sea farms was then unwrapped by the Flynn's method (Flynn, 1997).

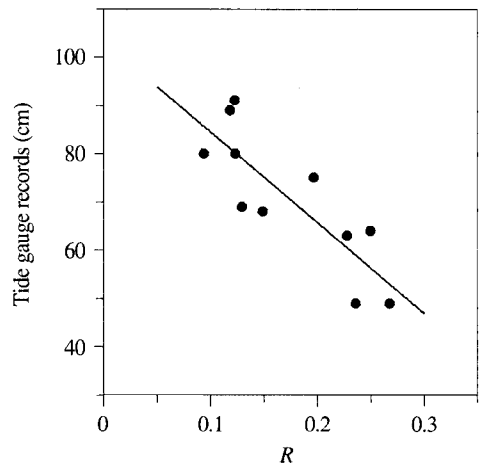

Fig. 3. Tide height versus a normalized image intensity (R).

3. Results and Discussion

From 21 interferograms, the instantaneous sea level were estimated for the first time. We first converted the differential phase into smooth surface by fitting to a second order 2-D polynomial planes. In the 2-D polynomial fitting, we used pixels of high coherence (>0.4) only. The fitted surface presents the relative sea level change with respect to the sea level on the master scene acquisition. The fitted surface was then converted to an absolute sea level by adding the wrapping counts determined through the proposed method. The correlation coefficient between the radar measurements and tide gauge data was 0.96 with an r.m.s. error of 6.0 cm (Fig. 4). The possible error sources include phase noise error (up to 1.8 cm) and the tide gauge measurements, which was not on-site measurements but

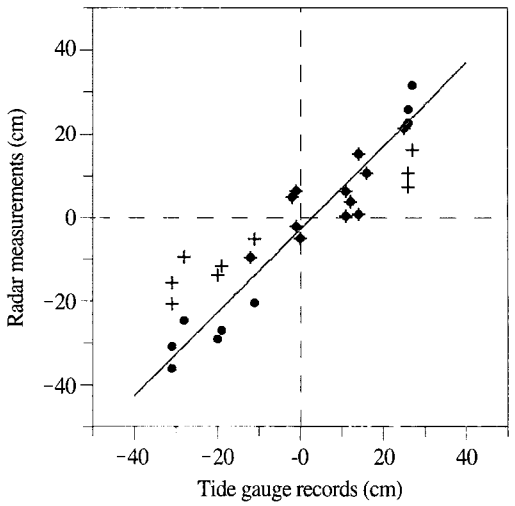

Fig. 4. Plot of tide gauge records versus radar measurements. The crosses denote the ambiguity of the tide heights occurred in image intensity analysis, while the dots present the final results.

5 km away from the test site, causing an error of up to 5 cm. The normalized image intensity resulted in broad range of wrapping counts in some data. In such cases, we selected the value favorable to tide gauge data. Thus unwrapping is so far a serious problem, but this problem can be alleviated if a calibrated image is used. The results demonstrate that the radar interferometry combined with signal intensity analysis is applicable to sea level measurement.

From the results, we can give answers to questions raised by Alsdorf (2002). First, can large perpendicular baselines at L-band yield water level changes? Scatterers on the water surface could be considered as pointwise scatterers, thus it would be coherent with unlimited baselines (Ferretti *et al.*, 2001). Although the critical baseline for JERS-1 L-band SAR system is about 7.5 km (Massonnet *et al.*, 1998), the baselines used in our research were as long as 2 km and formed interferometric phase extremely well. Therefore the answer must be yes to his first question. Second, is L-band coherence a function of temporal baseline? Oyster growing would affect coherence besides ocean wind and wave action. Nevertheless we were able to obtain several interferometric pairs with over one-year temporal baseline. Third, does L-band coherence vary with scatterer density? The averaged coherence in the sea farms was 0.32 (with a maximum of 0.57 and a minimum of 0.16) in a 5×15 sub-window. Using IKONOS image acquired on February 9, 2001, the arrayed structures of oyster farms were delineate and the density was evaluated. It appears that the coherence is affected by a direction of array as well as scatterer density.

JPL AIRSAR data was acquired over the study area with XTI1 mode (L-band and P-band polarimetric mode, C-band TOPSAR mode) on September 30, 2000, as a PACRIM-II experiment. The data is being processed by JPL, and is expected to provide valuable information on the study.

4. Conclusions

The radar signals from sea farms could be considered as double-bouncing returns by the vertical and horizontal bars because the interferometric phase distinctively differs from the differential phase observed on land. Considering 21 interferograms maintaining high coherence, a temporal and geometrical baseline did not affect the coherence at large. A large baseline (up to 2 km) can be tolerated in case of a short temporal baseline, conversely a large temporal baseline (about 1 year) can be accommodated in case of a short orbital baseline. A normalized radar image intensity was used to resolve the ambiguity problem of wrapped phase. Comparison of the radar measurements with the tide gauge records yielded a correlation coefficient of 0.96 with an r.m.s. error of 6.0 cm. Although a peculiar structure such as vertical and horizontal bars in array is required, the results demonstrate that SAR is promising for sea level observation in the near coast.

The intensity image of JERS-1 SAR was not fully calibrated, and therefore we improvised a relative normalization method. Calibrated L-band SAR data such as ALOS PALSAR will produce better results in the future works. This SAR technique can be applied to a remote site, for example, Antarctic coast, in association with satellite altimetry.

References

Alsdorf, D.E., J.M. Melack, T. Dunne, L.A.K. Mertes, L.L. Hess and L.C. Smith, 2000. Interferometric radar measurements of water level changes on the Amazon flood plain, *Nature*, 404: 174-177.

Alsdorf, D.E., L.C. Smith and M. Melack, 2001a. Amazon Floodplain Water Level Changes Measured with Interferometric SIR-C Radar, *IEEE Transactions on Geoscience and Remote*

Sensing, 39(2): 423-431.

Alsdorf, D.E., C. Birkett, T. Dunne, J. M. Melack and L.L. Hess, 2001b. Water Level Changes in a Large Amazon Lake Measured with Spaceborne Radar Interferometry and Altimetry, *Geophysical Research Letters*, 28(14): 2671-2674.

Alsdorf, D.E., 2002. Interferometric SAR observations of water level changes: Potential targets for future repeat-pass AIRSAR missions, *Proc. of the 2002 AIRSAR Earth Science Applications Workshop* [CD-ROM], March 4-6, 2002, Pasadena, California, JPL Propulsion Laboratory.

Amelung, F., D. L. Galloway, J. W. Bell, H. A. Zebker and R. J. Laczniak, 1999. Sensing the ups and downs of Las Vegas: InSAR reveals structural control of land subsidence and aquifersystem deformation, *Geology*, 27(6): 483-486.

Ferretti, A., C. Prati and F. Rocca, 2001. Permanent Scatterers in SAR Interferometry, *IEEE Transactions on Geoscience and Remote Sensing*, 39(1): 8-20.

Flynn, T.J., 1997. Two-dimensional phase unwrapping with minimum weighted discontinuity, *Journal of Optical Society of America A*, 14(10): 2692-2701.

Kim, S.W., C.W. Lee and J.S. Won, 2002a. Characteristics of the SAR images and interferometric phase over oyster sea farming site, *Korean Journal of Remote Sensing* (Korean ed.), 18(4): 209-220.

Kim, S.W., C.W. Lee, J.S. Won and K.D. Min, 2002b. Estimation of the subsidence rate of reclaimed coastal land using L-band SAR differential interferometry, *Geophysical Research Letters*, (in review).

Massonnet D. and K.L. Feigl, 1998. Radar interferometry and its application to changes in the earth's surface, *Review of Geophysics*, 36: 441-500.

Massonnet D., M. Rossi, C. Carmona, F. Adragna, G. Peltzer, K. Fiegl and T. Rabaute, 1993. The displacement field of the Landers earthquake mapped by radar interferometry, *Nature*, 364: 138-142.

Robinson, I.S., 1994. *Sattllite oceanography*, John Wiley & Sons Ltd., New York, USA.

Ross, S.M., 1987. *Introduction to Probability and Statistics for Engineers and Scientists*, John Wiley & Sons, Inc., New York, USA.

Sandwell, D.T., L. Sichoix, D. Agnew, Y. Bock and J-B. Minster, 2000. Near real-time radar interferometry of the Mw 7.1 Hector Mine Earthquake, *Geophysical Research Letters*, 2(19): 3101-3104.

Schmullius C.C. and D.L. Evans, 1997. Synthetic aperture radar (SAR) frequency and polarization requirements for applications in ecology, geology, hydrology, and oceanography: a tabular status quo after SIR-C/X-SAR, *Int. J. Remote sensing*, 18(13): 2713-2722.

Shimada, M., 1998, *User's Guide to NASDA's SAR products*, Earth Observation research center National Space Development Agency of Japan, pp. 1-24.